

# Hydride Attack on a Coordinated Ferric Nitrosyl: Experimental and DFT Evidence for the Formation of a Heme Model–HNO Derivative

Erwin G. Abucayon,<sup>†</sup> Rahul L. Khade,<sup>‡</sup> Douglas R. Powell,<sup>†</sup> Yong Zhang,<sup>\*,‡</sup> and George B. Richter-Addo<sup>\*,†</sup>

<sup>†</sup>Department of Chemistry and Biochemistry, University of Oklahoma, Norman, Oklahoma 73019, United States

<sup>‡</sup>Department of Biomedical Engineering, Chemistry and Biological Sciences, Stevens Institute of Technology, Castle Point on Hudson, Hoboken, New Jersey 07030, United States

**S** Supporting Information

**ABSTRACT:** Heme–HNO species are crucial intermediates in several biological processes. To date, no well-defined Fe heme–HNO model compounds have been reported. Hydride attack on the cationic ferric [(OEP)Fe(NO)(5-MeIm)]OTf (OEP = octaethylporphyrinato dianion) generates an Fe–HNO product that has been characterized by IR and <sup>1</sup>H NMR spectroscopy. Results of DFT calculations reveal a direct attack of the hydride on the N atom of the coordinated ferric nitrosyl.

HNO is the conjugate acid of the product of one-electron reduction of NO. HNO elicits biological responses such as vasodilation and cardioprotection, but unlike NO, it readily dimerizes to generate N<sub>2</sub>O and water.<sup>1</sup> It is also present as a heme ligand in heme–HNO intermediates in important biological processes such as NO detoxification by fungal cytochrome P450 nitric oxide reductase (P450nor),<sup>2,3</sup> and in the reaction cycles of cytochrome *c* nitrite reductase (ccNiR)<sup>4,5</sup> and hydroxylamine oxidoreductase.<sup>6</sup> Outstanding work by Farmer has resulted in the spectroscopic characterization of several heme protein–HNO adducts.<sup>7</sup> Coordination compounds with HNO ligands have been reviewed.<sup>1,8,9</sup>

Heme–HNO intermediates in biology may be generated either from proton attack at reduced nitrosyl moieties, such as proposed in ccNiR,<sup>4,5</sup> or from hydride attack at the ferric nitrosyl center in P450nor.<sup>2</sup> Elegant work by Ryan,<sup>10</sup> Meyer,<sup>11</sup> and others has shown that (por)Fe–HNO species are likely intermediates during the electrochemical reductions of ferrous–NO porphyrins in the presence of protons to yield Fe–NH<sub>2</sub>OH derivatives and NH<sub>3</sub>. A similar inference of an Fe–HNO species was based on UV–vis spectroscopy,<sup>12</sup> but no spectral signals to verify the presence of bound HNO were obtained. The related anionic five-coordinate [(TFPPBr<sub>8</sub>)Fe(NO)]<sup>−</sup> (TFPPBr<sub>8</sub> = octabromo[tetrakis(pentafluorophenyl)]porphyrinato dianion) complex has been isolated,<sup>13</sup> and its crystal structure has been determined.<sup>14</sup>

Although nucleophilic attack by hydride (H<sup>−</sup>) at a ferric–NO moiety is a key step in NO detoxification by fungal P450nor en route to hyponitrite and N<sub>2</sub>O formation, there are no well-defined examples of this nucleophilic reaction type in Fe heme models. In fact, there are only two known examples of hydride attack at metal-coordinated nitrosyls. In 2001, Sellman reported hydride attack on [(py(by)S<sub>4</sub>)RuNO]<sup>+</sup> to give the

Ru–HNO product,<sup>15</sup> and in 2004 we reported hydride attack on [(TTP)Ru(NO)(1-MeIm)]<sup>+</sup> (TTP = tetratolylporphyrinato dianion) to give the Ru–HNO derivative.<sup>16</sup> Prior to our current work, the latter was the only clearly defined heme model–HNO compound reported for any metal. Indeed, despite the importance of heme–HNO intermediates in biology, it is surprising that there are no reports of well-characterized Fe heme model–HNO compounds. Some density functional theory (DFT) calculations on (porphine)-Fe–HNO species have been reported.<sup>17,18</sup> In this paper, we report the first experimental generation of a heme model–HNO complex from hydride attack at a ferric nitrosyl moiety and the results of DFT calculations to probe the reaction pathway to form the heme model–HNO adduct.

Our selection of the ferric nitrosyl reagent [(OEP)Fe(NO)(5-MeIm)]OTf ( $\nu_{\text{NO}} = 1895 \text{ cm}^{-1}$ ; KBr pellet) was based on our observation that unlike most ferric nitrosyls, this cationic precursor can be prepared in analytically pure form (see the Supporting Information (SI)). The molecular structure of the cation, shown in Figure 1, confirms the identity of this formally {FeNO}<sup>6</sup> precursor with a near-linear Fe–NO moiety. Hydride attack on this ferric nitrosyl cation was monitored by IR and <sup>1</sup>H

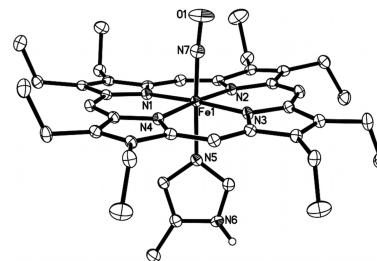
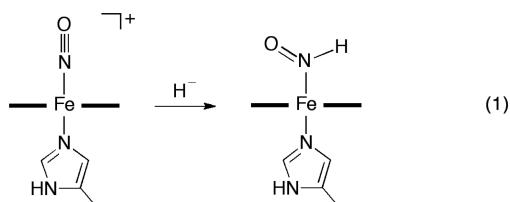


**Figure 1.** Ordered molecular structure of the cation of [(OEP)Fe(NO)(5-MeIm)]OTf, with thermal ellipsoids shown at 50% probability. The hydrogen atoms (except for the imidazole N6 proton) and the anion have been omitted for clarity. The imidazole N6 proton is hydrogen-bonded to an O atom of the triflate anion, with N6...O(OTf) = 2.880(2) Å (not shown). Selected bond lengths (Å) and angles (deg): Fe1–N7 = 1.6437(16), N7–O1 = 1.152(2), Fe1–N5 = 1.9823(15), Fe1–N(por) = 2.0039(14)–2.0119(14), ∠Fe1–N7–O1 = 175.38(16).

Received: November 16, 2015

Published: December 17, 2015

NMR spectroscopy, and both point to the formation of the ferrous (OEP)Fe(HNO)(5-MeIm) product as shown in eq 1.



Addition of 1.5 equiv of the hydride reagent  $[\text{NBu}_4]\text{BH}_4$  to a solution of  $[(\text{OEP})\text{Fe}(\text{NO})(5\text{-MeIm})]\text{OTf}$  (9.5 mg, 0.011 mmol) in  $\text{CHCl}_3$  (1.5 mL) at  $-20^\circ\text{C}$  resulted in a decrease of the precursor  $\nu_{\text{NO}}$  band in the IR spectrum at  $1912\text{ cm}^{-1}$  with the concomitant formation of a medium-intensity band at  $1383\text{ cm}^{-1}$  (Figure 2a).

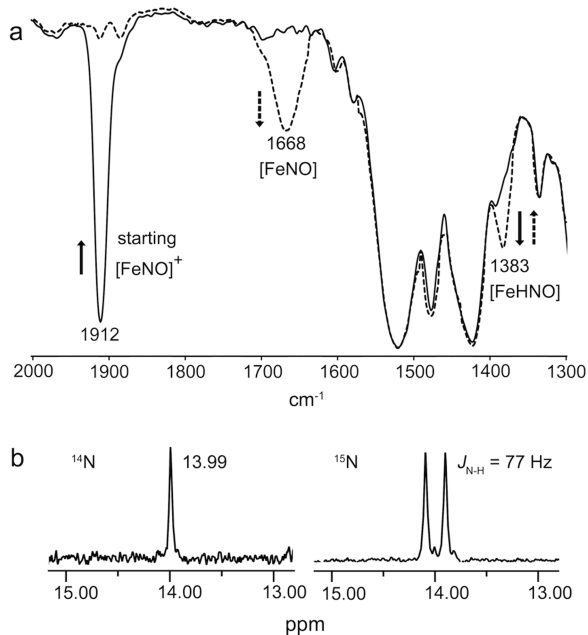


**Figure 2.** Spectroscopic characterization of the bound HNO ligand in  $(\text{OEP})\text{Fe}(\text{HNO})(5\text{-MeIm})$ . (a) IR spectrum showing the formation of the  $\nu_{\text{NO}}$  band at  $1383\text{ cm}^{-1}$  (dashed line) upon hydride addition to the cationic precursor ( $\nu_{\text{NO}} = 1912\text{ cm}^{-1}$ ). The new band at  $1383\text{ cm}^{-1}$  slowly converts to a band at  $1668\text{ cm}^{-1}$ . (b)  $^1\text{H}$  NMR spectrum showing the formation of the HNO ligand at  $\delta = 13.99\text{ ppm}$  (left) and the  $J_{\text{NH}}$  coupling for the  $\text{H}^{15}\text{NO}$  derivative (right).

Employing the  $^{15}\text{N}$ -labeled precursor  $[(\text{OEP})\text{Fe}(^{15}\text{NO})(5\text{-MeIm})]\text{OTf}$  ( $\nu_{^{15}\text{NO}} = 1874\text{ cm}^{-1}$ ) for the reaction shifted this isotope-sensitive band from  $1383\text{ cm}^{-1}$  in the unlabeled product to  $1360\text{ cm}^{-1}$  (Figure S1), confirming the assignment of this new band to  $\nu_{\text{NO}}$  of the product. Addition of  $\text{PPh}_3$  as an HNO trap<sup>19</sup> to the product mixture at  $-20^\circ\text{C}$  resulted in the generation of  $\text{HN}=\text{PPh}_3$  ( $m/z$  278.1101) and  $\text{O}=\text{PPh}_3$  ( $m/z$  279.0937) as determined by electrospray ionization mass spectrometry, confirming the presence of HNO in the product of eq 1. The  $\nu_{\text{NO}}$  band at  $1383\text{ cm}^{-1}$  for this ferrous porphyrin derivative is in the range observed for non-porphyrin metal–HNO complexes ( $1335\text{--}1493\text{ cm}^{-1}$ )<sup>8</sup> and is similar to the  $\nu_{\text{NO}}$  determined for  $\text{Mb}(\text{HNO})$  ( $1385\text{ cm}^{-1}$ ).<sup>20</sup> This new  $1383\text{ cm}^{-1}$  band assigned to  $(\text{OEP})\text{Fe}(\text{HNO})(5\text{-MeIm})$  slowly converts, even at  $-20^\circ\text{C}$ , to the  $\nu_{\text{NO}}$  band at  $1668\text{ cm}^{-1}$

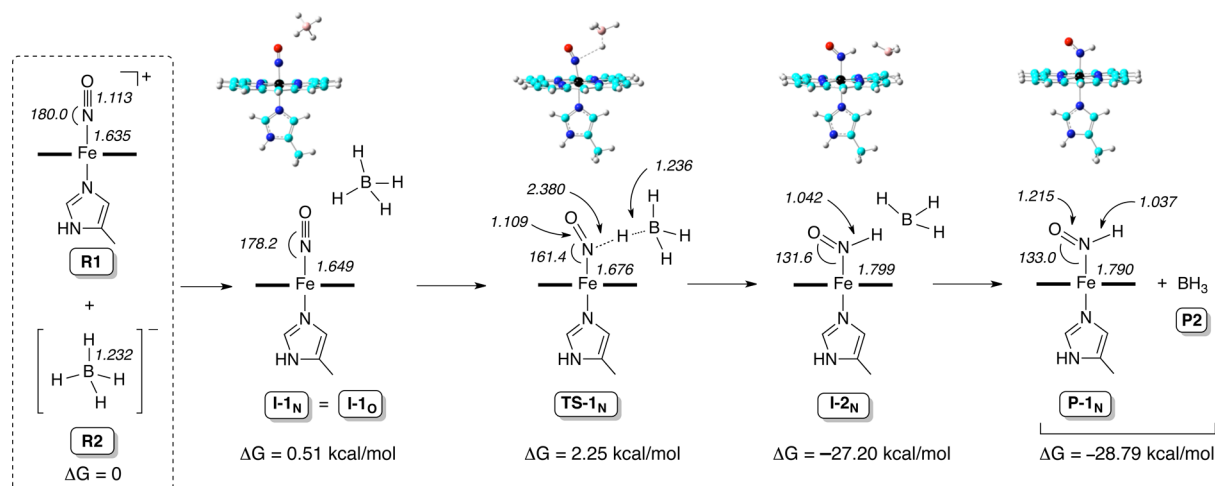
assigned to the known five-coordinate complex  $(\text{OEP})\text{Fe}(\text{NO})$  in an overall yield of the latter ferrous nitrosyl, based on the precursor ferric nitrosyl cation ( $\nu_{\text{NO}} = 1912\text{ cm}^{-1}$ ; Figure 2a), of  $\sim 85\%$  as judged by IR spectroscopy.

Monitoring of the hydride addition to the ferric nitrosyl cation (eq 1) in  $\text{CDCl}_3$  at  $-20^\circ\text{C}$  by  $^1\text{H}$  NMR spectroscopy revealed the appearance of a new peak at  $13.99\text{ ppm}$  assigned to the bound HNO of the product of eq 1 (Figure 2b). When the  $^{15}\text{N}$ -labeled nitrosyl cation precursor was used for the reaction, the new peak split into a doublet with a coupling constant ( $J_{\text{NH}}$ ) of  $77\text{ Hz}$ . The downfield  $^1\text{H}$  NMR chemical shift of  $13.99\text{ ppm}$  for the bound HNO ligand in  $(\text{OEP})\text{Fe}(\text{HNO})(5\text{-MeIm})$  is close to those determined for ferrous heme globin–HNO adducts ( $14.63\text{--}15.53\text{ ppm}$ ) by Farmer and co-workers.<sup>7</sup> The magnitude of  $J_{\text{NH}}$  ( $77\text{ Hz}$ ) is typical for N-coordinated HNO ligands and consistent with the direct attachment of the proton to the N atom of the HNO moiety.<sup>21</sup> Examination of the  $^1\text{H}$  NMR spectrum (Figure 2b) revealed the presence of a minor species ( $\sim 9\%$  of the HNO signal) with  $\delta = 13.91\text{ ppm}$  and  $J_{\text{NH}} = 74\text{ Hz}$ , which we tentatively assign as a rotational isomer. We note that similar minor signals have been observed in some heme protein–HNO adducts.<sup>7</sup> Consistent with the IR spectral results, the  $(\text{OEP})\text{Fe}(\text{HNO})(5\text{-MeIm})$  compound decomposes slowly even at  $-20^\circ\text{C}$ , and we have identified  $\text{H}_2$  as a byproduct of this decomposition on the basis of its characteristic  $^1\text{H}$  NMR chemical shift<sup>22</sup> at  $4.62\text{ ppm}$  in  $\text{CDCl}_3$ . The  $^1\text{H}$  signal for the bound Fe–HNO persists in the product mixture for at least 2–4 h at  $-20^\circ\text{C}$  and integrates to a yield of  $\sim 11\%$  at this temperature. The  $\text{H}_2$  product is also present in the headspace after the reaction as determined by  $^1\text{H}$  NMR spectroscopy and gas chromatography (Figure S3), consistent with a previous report by Ryan.<sup>10</sup>

Importantly, our results represent the first experimental demonstration of hydride attack on a coordinated Fe heme nitrosyl to give a heme model–HNO compound and the first direct spectroscopic characterization of a bound HNO ligand in an Fe heme model.

We investigated the mechanism of hydride attack on the ferric nitrosyl cation (eq 1) using DFT calculations. Three different DFT methods were used (see the SI), and all three methods showed basically the same trends. The mpW1PW91 method was previously found to yield excellent predictions of mechanistic properties,<sup>23–25</sup> and hence, results from this method are shown in Scheme 1 and discussed here.

For the isolated nitrosyl cation  $[(\text{P})\text{Fe}(\text{NO})(5\text{-MeIm})]^+$  (reactant 1; R1 in Scheme 1; P = unsubstituted porphine macrocycle), the nitrosyl N atom has a large positive charge of  $0.705e$ , whereas the O atom has a charge of  $-0.040e$ . This suggests that the N atom should be more easily attacked (compared with the O atom) by the incoming negatively charged hydride from  $\text{BH}_4^-$  (reactant 2; R2) to form the HNO product rather than the NOH product. Interestingly, we find that for the first intermediate formed from the intermolecular interaction between R1 and R2, all of the trials that placed the hydride closer to the nitrosyl N of R1 than the O atom, to form the potential  $\text{I-1}_\text{N}$  intermediate, resulted in the same structure as the intermediate  $\text{I-1}_\text{O}$  (i.e.,  $\text{I-1}_\text{N} = \text{I-1}_\text{O}$ ; Scheme 1),<sup>26</sup> with the distance between the hydride (H) to be transferred and the O atom ( $2.738\text{ \AA}$ ) being shorter than that for the nitrosyl N atom ( $3.353\text{ \AA}$ ). This is probably due to repulsion between the strong negative charge of  $\text{BH}_4^-$  and the porphine ring if they are too close. This result is reminiscent of that obtained from

Scheme 1. DFT-Calculated N-Pathway for Hydride Addition to the [(P)Fe(NO)(5-MeIm)]<sup>+</sup> CationTable 1. <sup>1</sup>H NMR Chemical Shifts (in ppm) and NO Vibrational Stretching Frequencies (in cm<sup>-1</sup>) for the Bound HNO/NOH Ligands

system	method	$\delta_{\text{H}}$	$\nu_{\text{NO}}$
(OEP)Fe(HNO)(5-MeIm)	expt	13.99	1383
(P)Fe(HNO)(5-MeIm) (P-1 <sub>N</sub> )	calc	13.91	1375
(P)Fe(NOHD <sub>own</sub> )(5-MeIm) (P-1 <sub>O</sub> ) ( <i>trans</i> ) <sup>a</sup>	calc	11.92	1005
(P)Fe(NOHD <sub>own</sub> )(5-MeIm) (P-1 <sub>O</sub> ) ( <i>cis</i> ) <sup>a</sup>	calc	11.36	992
(P)Fe(NOHD <sub>up</sub> )(5-MeIm)	calc	13.54	955

<sup>a</sup>NO *trans/cis* with respect to the Me substituent of 5-MeIm. As this *trans/cis* effect is relatively small, only the *trans* isomer for the NOH<sub>Up</sub> conformation was studied here. The Down/Up conformations are for the H pointing to and away from the porphyrin ring, respectively.

quantum-chemical investigations of hydride attack on the NO moiety in the heme protein P450nor.<sup>3</sup>

Since both the N and O atoms of the nitrosyl moiety in the first intermediate I-1<sub>N/O</sub> may in principle accept the transferred hydride from borohydride, we investigated both the N- and O-pathways for hydride addition to the bound nitrosyl of the common intermediate I-1<sub>N/O</sub> (Scheme S1). Relative electronic energy ( $\Delta E_{\text{SCF}}$ ), zero-point-energy-corrected electronic energy ( $\Delta E_{\text{SCF+ZPE}}$ ), enthalpy ( $\Delta H$ ), and Gibbs free energy ( $\Delta G$ ) results with respect to reactants for both the N- and O-pathways are shown in Table S8. All of the energy results show the same trend, with the formation of the HNO complex (i.e., the N-pathway) having a much lower kinetic barrier and more favorable thermodynamic driving force.<sup>27</sup> Optimized structures of the lowest-energy conformations of key species for the N-pathway are shown in Scheme 1, as are selected bond lengths and angles for the complexes.

Hydride attack along the N-pathway (Scheme 1) proceeds via the transition state complex TS-1<sub>N</sub>, in which the hydride to be transferred is positioned between the nitrosyl N atom and boron. The geometric parameters (Table S11) show that this TS-1<sub>N</sub> geometry is more similar to the reactants than the products, suggesting an early transition state for a facile reaction, as observed experimentally. Charge analysis for TS-1<sub>N</sub> (Table S12) showed that both the boron atom and the hydride to be transferred possess negative charges ( $-0.671e$  and  $-0.073e$ , respectively) to help repel each other to break the B-H bond in the borohydride. The B-H bond cleavage generates the second intermediate I-2<sub>N</sub>, followed by complete dissociation of the BH<sub>3</sub> molecule to form the products P-1<sub>N</sub> and P2.

In contrast, reaction along the O-pathway (bottom of Scheme S1) generates the first transition state TS-1<sub>O</sub>, for which charge analysis showed opposite charges for the boron atom ( $-0.237e$ ) and the hydride to be transferred ( $0.243e$ ). This results in an attraction between B and H, and hinders the bond-breaking process needed for the hydride addition reaction to proceed via the O-pathway.

Further evidence for the formation of the Fe-HNO product rather than the Fe-NOH product comes from calculations of the spectral properties of these adducts (Table 1). The NMR properties were calculated using the B3LYP method with solvent effects (see the SI), similar to the approach used previously to study <sup>1</sup>H NMR chemical shifts in various organometallic complexes.<sup>28</sup> Compared to the experimental values for (OEP)Fe(HNO)(5-MeIm), our results for (P)Fe(HNO)(5-MeIm) (P-1<sub>N</sub> in Scheme 1) have errors of only 0.08 ppm (<sup>1</sup>H NMR) and 6 cm<sup>-1</sup> (IR). In contrast, the calculations for the various (P)Fe(NOHD<sub>up</sub>)(5-MeIm) conformations yield much greater errors of  $\sim 2$  ppm and/or up to 400 cm<sup>-1</sup>.

In summary, this report represents the first experimental demonstration of hydride attack on a coordinated nitrosyl of a synthetic ferric-NO porphyrin and the first spectral characterization of a bound HNO group in an Fe heme model. DFT calculations are consistent with direct hydride attack at the nitrosyl N atom in the precursor ferric nitrosyl porphyrin. Experiments to determine the fundamental chemistry patterns of heme model Fe-HNO moieties are currently underway.

## ■ ASSOCIATED CONTENT

### Supporting Information

The Supporting Information is available free of charge on the ACS Publications website at DOI: 10.1021/jacs.5b12008.

Experimental and computational details (PDF)  
Crystallographic data (CIF)

## AUTHOR INFORMATION

### Corresponding Authors

\*yong.zhang@stevens.edu (DFT)

\*grichteraddo@ou.edu (experimental)

### Notes

The authors declare no competing financial interest.

## ACKNOWLEDGMENTS

G.B.R.-A. thanks the National Science Foundation (CHE-1213674) and Y.Z. thanks the National Institutes of Health (GM085774) for financial support. We thank Dr. Ralph Tanner (OU) for assistance with the GC measurements.

## REFERENCES

- (1) Miranda, K. M. *Coord. Chem. Rev.* **2005**, *249*, 433–455.
- (2) Daiber, A.; Shoun, H.; Ullrich, V. *J. Inorg. Biochem.* **2005**, *99*, 185–193.
- (3) Kramos, B.; Menyhard, D. K.; Olah, J. *J. Phys. Chem. B* **2012**, *116*, 872–885.
- (4) Einsle, O.; Messerschmidt, A.; Huber, R.; Kroneck, P. M. H.; Neese, F. *J. Am. Chem. Soc.* **2002**, *124*, 11737–11745.
- (5) Bykov, D.; Neese, F. *Inorg. Chem.* **2015**, *54*, 9303–9316.
- (6) Cabail, M. Z.; Kostera, J.; Pacheco, A. A. *Inorg. Chem.* **2005**, *44*, 225–231.
- (7) Kumar, M. R.; Pervitsky, D.; Chen, L.; Poulos, T.; Kundu, S.; Hargrove, M. S.; Rivera, E. J.; Diaz, A.; Colon, J. L.; Farmer, P. J. *Biochemistry* **2009**, *48*, 5018–5025.
- (8) Farmer, P. J.; Sulc, F. *J. Inorg. Biochem.* **2005**, *99*, 166–184.
- (9) Doctorovich, F.; Bikiel, D.; Pellegrino, J.; Suarez, S. A.; Larsen, A.; Marti, M. A. *Coord. Chem. Rev.* **2011**, *255*, 2764–2784.
- (10) Choi, I.-K.; Liu, Y.; Feng, D.; Paeng, K.-J.; Ryan, M. D. *Inorg. Chem.* **1991**, *30*, 1832–1839.
- (11) Barley, M. H.; Takeuchi, K. J.; Meyer, T. J. *J. Am. Chem. Soc.* **1986**, *108*, 5876–5885.
- (12) Goodrich, L. E.; Roy, S.; Alp, E. E.; Zhao, J. Y.; Hu, M. Y.; Lehnert, N. *Inorg. Chem.* **2013**, *52*, 7766–7780.
- (13) Pellegrino, J.; Bari, S. E.; Bikiel, D. E.; Doctorovich, F. *J. Am. Chem. Soc.* **2010**, *132*, 989–995.
- (14) Hu, B.; Li, J. F. *Angew. Chem., Int. Ed.* **2015**, *54*, 10579–10582.
- (15) Sellmann, D.; Gottschalk-Gaudig, T.; Haussinger, D.; Heinemann, F. W.; Hess, B. A. *Chem. - Eur. J.* **2001**, *7*, 2099–2103.
- (16) Lee, J.; Richter-Addo, G. B. *J. Inorg. Biochem.* **2004**, *98*, 1247–1250.
- (17) Linder, D. P.; Rodgers, K. R. *Inorg. Chem.* **2005**, *44*, 8259–8264.
- (18) Zhang, Y. *J. Inorg. Biochem.* **2013**, *118*, 191–200.
- (19) Reisz, J. A.; Zink, C. N.; King, S. B. *J. Am. Chem. Soc.* **2011**, *133*, 11675–11685.
- (20) Immoos, C. E.; Sulc, F.; Farmer, P. J.; Czarnecki, K.; Bocian, D. F.; Levina, A.; Aitken, J. B.; Armstrong, R. S.; Lay, P. A. *J. Am. Chem. Soc.* **2005**, *127*, 814–815.
- (21) Southern, J. S.; Green, M. T.; Hillhouse, G. L.; Guzei, I. A.; Rheingold, A. L. *Inorg. Chem.* **2001**, *40*, 6039–6046.
- (22) Fulmer, G. R.; Miller, A. J. M.; Sherden, N. H.; Gottlieb, H. E.; Nudelman, A.; Stoltz, B. M.; Bercaw, J. E.; Goldberg, K. I. *Organometallics* **2010**, *29*, 2176–2179.
- (23) Michael, M. A.; Pizzella, G.; Yang, L.; Shi, Y. L.; Evangelou, T.; Burke, D. T.; Zhang, Y. *J. Phys. Chem. Lett.* **2014**, *5*, 1022–1026.
- (24) Zhang, Y.; Guo, Z. J.; You, X. Z. *J. Am. Chem. Soc.* **2001**, *123*, 9378–9387.
- (25) The energy difference between perpendicular and parallel axial planes in computed (P)Fe(N(H)O)(ligand) complexes is negligible,<sup>17</sup> and only the parallel orientations are shown here.
- (26) The computed Fe–N and Fe–NO geometries of **I-1<sub>N/O</sub>**, namely, [(P)Fe(NO)(S-MeIm)][BH<sub>4</sub>], more closely match that of experimental [(OEP)Fe(NO)(S-MeIm)]OTf than that of isolated R1.
- (27) Interestingly, these data are also consistent with results from a previous quantum-chemical study of hydride attack on the nitrosyl of a ferric heme thiolate as a model for P450<sub>nor</sub>.<sup>3</sup>
- (28) Zhang, Y.; Lewis, J. C.; Bergman, R. G.; Ellman, J. A.; Oldfield, E. *Organometallics* **2006**, *25*, 3515–3519.